Solution design for Low Fluorine Trifluoroacetate route to $YBa_2Cu_3O_7$ films

X. Palmer[1], C. Pop[1], H. Eloussifi[2,3], B.Villarejo[1], P. Roura[2], J. Farjas[2], A. Calleja[4], A. Palau[1] X. Obradors[1], T. Puig[1], S. Ricart[1]

[1] Institut de Ciència de Materials de Barcelona (CSIC), Campus UAB, 08193 Bellaterra, Spain.
[2] Departament de Fisica, Universitat de Girona, Campus Montilivi, 17017 Girona, Spain.
[3]Laboratoire de Chimie Inorganique, Faculté des Sciences de Sfax, Université de Sfax, BP 1171, 3000 Sfax, Tunisia
[4]OXOLUTIA, Edif. Eureka, Parc de Recerca de la UAB, Campus de la UAB, E-08193, Bellaterra, Spain

Abstract

We present our work in the preparation of metallorganic precursor solutions with reduced fluorine content, able to fulfill the requirements for high performance superconducting YBCO epitaxial layers as a promising approach to low cost and scalable coated conductors. Six different solutions using different quantities of fluorine and non-fluorine carboxylate precursors with a total amount of fluorine from 10% to 50% that of standard TFA solutions. For stabilization purposes different coordinating agents have been used and the solution rheology has been modified for proper substrate wetability. Thermal decomposition analysis and infrared spectroscopy performed directly in films, have revealed that the decomposition takes place in two consecutive stages around 265ºC and 310ºC respectively, and NMR analysis could unveil the chemical reactions taking place in the solution. Using the solutions with 20% of fluorine and upon optimization of the growth process parameters, YBCO layers with T_c and J_c(77K) of 90 K and 4 MA/cm^2 are obtained.

1. Introduction

Chemical solution deposition is a competitive technique to obtain epitaxial films. In particular, metal-organic decomposition has been established as the versatile methodology to grow low cost, scalable, high performance epitaxial $YBa_2Cu_3O_7$ films for coated conductors.[1–5]. The trifluoroacetate approach (TFA-MOD) has been the process mainly used for the preparation of YBCO layers [6]. This barium fluoride process, although currently used for industrial companies in the development of long-length biaxially textured coated conductors is still deeply studied, especially to better understand the underlying decomposition and growth mechanisms and be able to further improve growth rates, thickness, throughputs and performance[6]. This includes, among others, study of the deposition, evaporation, shrinkage and decomposition step, especially for thick layers and correlate them with the use of modified starting solutions [7,8]. In addition, the intermediate phase evolution and the nucleation and growth mechanisms for these modified solutions should be further analyzed to ensure best performance[9] . The modification of the solutions intends to reach more environmental friendly processes, enhanced thickness, planarized final HTS layers and generation of artificial pinning centers by growing nanocomposites [10,11]. For that reasons, different additives in the precursor solutions have been used in the form of organic molecules (monomers or polymers) or inorganic salts [12,13].

An important drawback in the use of TFA-YBCO solutions is the need to carefully control the water content of the solution and solution handling during preparation and storing to avoid environmental contamination. If the atmospheric absolute humidity exceeds 15 g/m^3 [14], inhomogeneous layers are obtained, and even cracks and buckling can be generated as a source of stress release before the decomposition step. An adequate solution design gives us a route to produce more environmentally robust solutions, as we will present in this work.

The use of fluorine in the TFA-MOD approach to YBCO layers is justified by two main reasons: the suppression of Barium Carbonate by formation of Barium Fluoride and the control of the growth process by HF evolving rate. By the here presented low fluorine solutions, we are able to accomplish with the new requirements concerning environmental safety by reduction of fluorine content. At the same time and the need of more robust designed metal-organic solutions (stable, reproducible, low water content and less hygroscopic) is also achieved. Previous studies have reported high performance layers from low fluorine solutions. [15,16]

By analyzing the behavior of the precursor salts in the solutions we demonstrate the possible use of different metal-trifluoroacetate salts ensuring an adequate combination of oxyfluorides after the decomposition step. The only requirement is the presence of enough overall fluorine in the precursor solution to produce the desired barium fluoride intermediates.

Solutions with low fluorine precursors with different solvents (methanol and propionic acid) and amount of additive (triethanolamine) have been stabilized and their rheology adapted to the deposition technique. NMR studies confirmed the conversion yield from acetates to propionates reactions taking place in the solution. Thermal decomposition analysis and IR spectroscopy performed directly in films, revealed that the decomposition of the precursor is completed at 350ºC and that no $BaCO_3$ is formed despite the fact that TFA salts decompose at high temperature. Upon optimization of growth process parameters, T_c and J_c(77K) of 90 K and 3-4 MA/cm^2 are reached for 300 nm layers.

2. Experimental details

Preparation and characterization of precursor solutions

Several Y, Ba, Cu metallorganic precursor solutions have been investigated with different contents of fluorine using several salts, solvents and concentration of additives. We identify (a) the standard TFA solution (with 100 % of fluorine content) using Yttrium, Barium and Copper trifluoroacetates as precursor salts and methanol as a single solvent and prepared as previously described [17], from those with a reduction of fluorine (listed below as (b)). In these fluorine reduced solutions, as is reported in Table 1, the precursors for low fluorine CSD process were yttrium trifluoroacetate (Y-TFA, Aldrich), yttrium acetate, barium trifluoroacetate (Ba-TFA, Aldrich), barium acetate (Ba-Ac, Aldrich), barium ethylhexanoate (Ba-Eth Aldrich) and/or copper acetate (Cu-Ac, Aldrich). A stoichiometric amount (Y:Ba:Cu = 1:2:3) of the precursors was dissolved in methanol (Solutions 1, 2, 3), methanol-propionic acid (CH_3OH:C_2H_5COOH = 75:25, solution 4) and propionic acid (solution 5). To these solutions triethanolamine (TEA, Aldrich) was added in 10%, 20% and 5% in volume (solutions 2, 3 and 4, respectively). Solution 6 was also prepared with just a 10% of fluorine as specified later.

The systematic analysis of these solutions were carried out by measuring the viscosity with a Haake RheoStress 600 rheometer (ordinary interval around 12-16 mPa·s at 22ºC), the contact angle with a DSA 100 analyzer (ordinary interval around 30º-35º on LAO substrates), the metal stoichiometry was checked by a volumetric assay and this was balanced to the 1:2:3 stoichiometry if necessary by the addition of metal-salts, and the water content in the solutions was measured by the Karl-Fischer method [18]. The thermogravimetric (TG) analysis was done with the TGA/DSC1 apparatus and the masses at room temperature where measured with the XS3DU balance, both from Mettler Toledo. Evolved Gas Analysis (EGA) was performed with a Spectra Quadrupole (Micro Vision Plus) from MKS Instruments. ^{1}H NMR and ^{13}C NMR spectra were recorded in CDCl3 on a Bruker ARX 300 (300 and 75.5 MHz) spectrometer,. Chemical shifts are given in ppm relative to TMS (^{1}H δ=0.0 ppm) or CDCl3 (^{13}C δ=77.0 ppm).

Thin film growth and characterization

The different metallorganic solutions were deposited by spin coating on (001) $LaAlO_3$ single crystal substrates (5mmx5mm) at a spinning rate of 6000 rpm for 2 min. The coatings were pyrolyzed in humid oxygen atmosphere to form precursor films. The heating rate was kept at 3 K/min in the temperature range from 100ºC to 500ºC. The humid gas was injected by bubbling the dry gas through deionized water (dew point 25ºC) into the furnace when the furnace temperature was higher than 110ºC. Subsequently, the YBCO precursor layers were crystallized at 820ºC in humid N_2/0.02% O_2. In the last stage the crystallized films were annealed at 450ºC for 4 h in a dry oxygen atmosphere.

Cross-section images were performed by using dual beam (SEM, FIB) Zeiss 1560 XB. Film thickness was determined either by surface profilometry or from FIB images and they were in the range of 250-350 nm.

X-ray diffractometry (XRD) $\theta/2\theta$ scans were performed on thin film samples using a Siemens D5000 diffractometer with Cu–Kα, λ =1.5418 Å. Phi scans were taken on a 2D general area detector diffraction system (GADDS) and a thin film diffractometer PANalytical model X'Pert PRO MRD. In both cases the X-ray beam wavelength was 1.5418 Å (Cu-Kα). IR spectroscopy was measured with a Spectrometer Perkin-Elmer Spectrum One in the energy range from 450-4000 cm^{-1}.

The inductive critical current density of the superconducting films, at self field, was determined from inductive measurements performed with a SQUID magnetometer and calculated accordingly with the Bean Model [19]. We have used the equation $J_c=3\Delta M/2a$ [20] valid for thin films, where $3\Delta M$ is the width of the saturated hysteresis loop at zero field and a is the sample radius.

Angular transport critical current measurements were carried out in a PPMS Quantum Design system. We patterned the sample with 30 μm width bridges, in the standard four probe geometry, by using standard photolithography with a Durham Magneto Optics Std MicroWriterTM. The transport current was sent parallel to the ab planes and the magnetic field was applied in the maximum Lorentz force configuration and rotated with an angle θ from the c axis (θ=180 º) to the ab plane (θ=0º). The critical current density was determined by using a 10 μVcm^{-1} criterion.

3. Results and discussion.

3.1. Solution formulation**.**

The fluorine in the metalloganic solutions is introduced by the fluorinated compounds used (trifluoroacetates, TFA). During the pyrolysis thermal treatment, the C-F bond is broken generating F anions or radicals that react with the Ba ions present in the mixture[21] thus generated the Ba, Y fluorinated compounds (Scheme1).

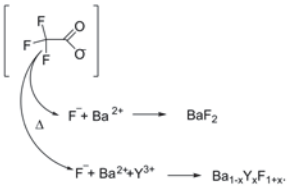

Scheme 1. Formation of fluorine compounds during thermal decomposition of metaloorganic salts.

The minimum amount of fluorine necessary for the formation of barium fluoride is deduced from this reaction and corresponds to 2 atoms of fluorine per 1 atom of barium. On the other hand, if we consider the formation of Barium, Yttrium Fluoride intermediate ($Ba_{1-x}Y_xF_{2+x}$ ($x \leq 0.5$) BYF) the maximum amount of fluorine necessary is 2,5 atoms of Fluorine per 1 atom of the solid solution ($Ba_{1-x}Y_x$). Therefore, taking into account the number of F atoms for all the TFA radicals present (i.e. 39 F atoms for the production of 1 equivalent of $YBa_2Cu_3O_7$), there exists a large excess of fluorine (39 atoms/2 Barium atoms) in the TFA solution.

If we only want to introduce the fluorine necessary to form the fluorine intermediates, we would require a 10% as compared to the 100 % assigned to the standard TFA solution. The reduction of the fluorine content in the solution can be done by combining fluorinated and non-fluorinated salts and we have investigated solutions with 10 %, 20 %, 30 % and 50 % of fluorine content.

By keeping just the $Y(TFA)_3$ metallorganic salt as the only salt containing fluorine in the solution, we get already 20% of F, i.e. much more than that required to form the desired (Barium,Ytrium) Fluoride.

In the attempt to further decrease the F content, a moderately stable solution could be prepared with 10% F. In this case a mixture of YTFA, YAc (1:1), 2 BaAc, and 3 CuAc in methanol/propionic acid solution have been prepared. Without further optimization, pyrolyzed layers with the similar crystalline phases than that in the case of all-TFA process were obtained although no Y was incorporated in the BaF_2 phase (see Fig. 1).

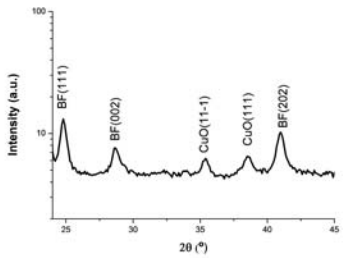

Figure 1.- XRD analysis of 10% Fluorine solution after pyrolysis.The expected barium fluorinated compound appeared. No barium carbonate formation is observed.

The different formulations for the low fluorine solutions are presented in Table 1.

Solution	Metalorganic salts 1:2:3 stoichiometry	Solvent	Conc.	[F content]	Additives
1	YAc, BaAc**, CuTFA**	**Methanol/acetic acid**	**1.5M**	**50%**	--
2	YAc, **BaTFA,** CuAc	**Methanol**	**1.5M**	**30%**	**10%TEA**
3	**YTFA,** BaEth, CuAc	**Methanol**	**1.5M**	**20%**	**20%TEA**
4	**YTFA,** BaAc, CuAc	**Methanol/Propionic acid**	**1.5-2M**	**20%**	**5%TEA**
5	**YTFA,** BaAc, CuAc	**Propionic acid**	**1M**	**20%**	--
6	**YTFA,** YAc, BaAc, CuAc	**Methanol/Propionic acid**	**1.5M**	**10%**	**5%TEA**

Table 1. Solutions with partial reduction of fluorine content.

Although there are different alternatives for the formulation of the starting metalorganic salts (see Scheme 2), in this work carboxylates are used for the following reasons: they are stable, commercially available and easy to prepare as compared to alkoxides, and they have lower carbon backbone content than acetylacetonates.

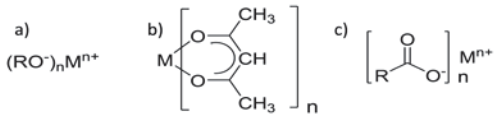

Scheme 2. Structures of the possible starting metalorganic salts. a) Alkoxide, b) acetylacetonate, c) carboxylate.

Taking into account the wetability requirements of the solutions for their deposition on the substrates, medium polar solvents like alcohols were used in their preparation. In the standard TFA approach the mostly used solvents are short chain alcohols like methanol or ethanol. In the preparation of low fluorine solutions methanol and short length carboxylic acids are used.

Metal acetates are carboxylates with low amount of carbon atoms in the chain. As a consequence, their solubility, even in short chain alcohols (medium polar solvents, with medium hydrogen bonding and low dispersion forces according to Hansen parameters [22]) will be rather low, particularly in the case of barium acetate. Then, taking into account the principle of "like dissolves like" [19] we need to use different additives or solvent mixtures, which are able to change solutes solubility parameters, for the stabilization of the solutions. These additives are mainly composed by carbon backbone molecules functionalized with alcohol, amine, ether carbonyl and carboxyl groups, isolated or mixed together [8,23]. Possible reactions of the additives with the YBCO precursors need to be considered because the stability of the resulting solutions

is clearly related to the solubility of products or complexes formed. After an initial screening of the stability of the solutions with a set of different additives and solvents, triethanolamine (TEA) and propionic acid in different quantities were used for the formulation of the solutions.

3.2 Solutions characterization.

All solutions presented with reduced fluorine content are stable for more than two weeks. The control of their rheological properties has enabled us to identify the requirements for the growth of YBCO superconducting layers. We should take into account, however, that these requirements will strongly defer depending on the deposition methodology intended to use (spin coating, dip coating, Ink Jet Printing) [24,25]

At this point, our concern is to reach homogeneous solutions with low water contents and rheological properties close to those from the standard TFA solution.

	Standard TFA solution	**Solution 1**	**Solution 2**	**Solution 3**	**Solution 4**	**Solution 5**	**Solution 6**
Viscosity (mPa.s)	2-5	4	12-14	12-14	9	1,5-2	6-7
Contact Angle	20	28	18-33	35	27	<10	25
Water content (%wt)	<1	1.3	<1	0.8	<2	0.5	<2
pH (in water)	2.5	5.8	7	7	4.2	4.2	4.2

Table 2. Characteristics of the TFA and low Fluorine solutions.

Rheological properties for all the solutions prepared have been evaluated for their use in CSD. Solutions with viscosity in the range of 10mPa.s. can easily be spin coated given rise to homogeneous pyrolysis. Solutions 2 and 3 with higher viscosities produced non homogeneous layers after deposition. The right values for contact angle are clearly dependent on the substrates used (single crystals or tapes). The values presented here corresponded to LAO single crystal as substrate. The solutions with contact angle <30 exhibit good wetting. The water content is an important parameter which we propose to be < 2%. Higher contents in water produced non homogenous layers after pyrolysis.

As it is well known, alcohol solutions are hygroscopic. This is because the hydrogen bond formations easily enable water absorption from the atmosphere. However a careful control of the preparation protocols and solution handling using inert atmosphere, keeps water content below 2%wt in all the cases. In our case we prepared the solutions under nitrogen atmosphere and the storage is in inert atmosphere in sealed vials at low temperature (4ºC). Using these precautions the solutions remain stable for three months without changes in their rheological properties.

3.3 Use of coordination compounds.

In the preparation of low fluorine solutions some additives or solvent mixtures are used for the stabilization of the solutions, to change solutes solubility parameters.

These ligands are mainly stabilizers for Copper. The formation of complexes of Cu(II) carboxylates with triethanolamine has been described previously by different groups [26,27].

It is important to know the minimum amount of ligand necessary for the stabilization of the non-fluorinated copper salt in the solution. Considering the stoichiometry of these complexes, two equivalents of TEA are necessary to stabilize two or three equivalents of copper depending on the coordination type. Then, for copper stabilization in the solution it would be necessary to use 10% of volume of TEA when no other competing ligands are present (Solutions **2** and **3**). However, we need up to 20% in volume of TEA to obtain a complete stable solution. That can be accounted for the Yttrium and Barium stabilization. Yttrium or Barium salts can interact with TEA forming stable and soluble intermediates as previously described[28].

Although solutions with a high content in TEA (around 20 % in volume in solution **3**) are promising and the first trials showed the production of good superconducting layers on LAO single crystal, its high viscosity (3 times higher than the standard TFA solution) is the reason for the irreproducibility problems observed in the deposition step. Layers with inhomogeneous pyrolysis and non-uniform distribution of liquid along the substrate are obtained after deposition by spin coating from this highly viscous solution.

Solutions **1** and **2** are adequate from the point of view of their rheological characteristics. However solution **4** and **5** are proposed as alternative to **2** due to their lower fluorine content. These latter solutions present a combination of aminoalcohol ligands and carboxylates like propionic acid. Carboxylic acids can act in two ways: a) forming carboxylates in the solution by scrambling with acetates giving salts with longer organic chains compatible with the methanol solvent and b) acting as a bidentate ligand interacting in the free positions of the structure (Scheme 3) and preventing water absorption [29].

To confirm some of these hypotheses we have studied their behavior by NMR studies. For that purpose and due to the difficulty to measure Copper-based solutions in NMR, we have prepared a solution containing only the binary mixture of Barium and Yttrium salts with the same combination of methanol, propionic acid and TEA used in Solution **4**. After evaporation of solvents until constant weight, ^{1}H- and ^{13}C-NMR spectrum of the remaining residues was obtained. From the ^{1}H-NMR spectra we observe the transformation of Barium acetate to Barium propionate in more than 80%. The quadruplet at 2.18 ppm (2H) and triplet at 0.98 ppm (3H) indicate the presence of the propionate moiety being the singlet at 1.89 ppm the remaining acetate. This is confirmed by ^{13}C-NMR spectra (singlet at 28.1 and 8.2 ppm for CH_3CH_2, and at 21.9 ppm for CH_3 from the acetate) where the presence of trifluoroacetate is also observed by the signals at 116.0 ppm and 161.7 ppm as quadruplets indicating the presence of fluorine atoms in the carbon chain (see Fig 2). This result confirms our initial assumption of the scrambling between propionate and acetate radicals in the solution. Therefore, the NMR study confirms the evolution from acetates to propionates and the permanence of fluorinated moiety in the layer.

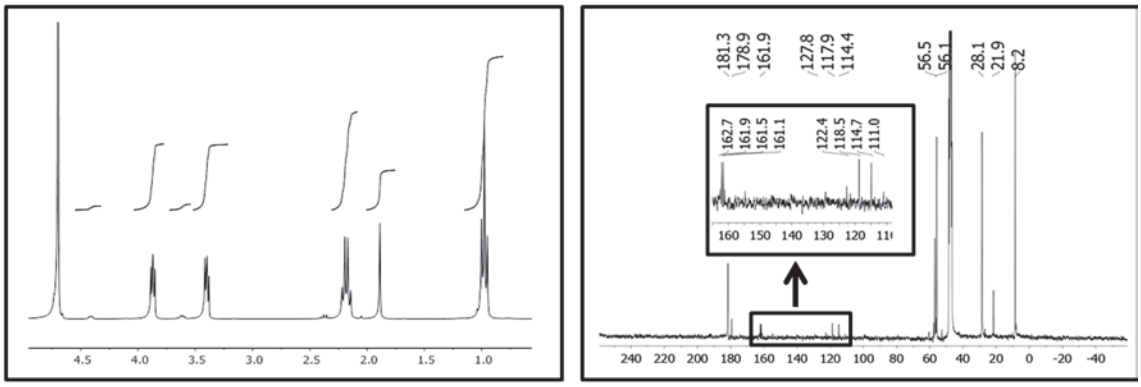

Figure 2. ^{1}H and ^{13}C-NMR spectra of the solution 3 with only Ba and Y salts. (inbox CF_3 and C-CF_3 signals).

Water is strongly absorbed during the deposition and drying (evaporation) process. The content of water increases very quickly for dried layers, because the evaporation of the solvent makes the highly hygroscopic salts to easily coordinate with hydroxyl groups. This process renders a safe handling quite difficult. In the case of all TFA solution 1, this phenomenon leads to the necessity to work in a controlled atmosphere with environmental absolute humidity below 15 gr/m^3 up to the pyrolysis process. When this value is surpassed the deposited layers strongly suffer an unwetability process accumulating the solution to the centre of the substrate.

We have observed that the use of additives can strongly inhibit the water absorption phenomenon occurring in the deposited layers. Figure 3 shows the rate of water absorption on deposited layers produced from solutions **4** and **5** and from the standard TFA solution. The measurements were carried out with a microbalance in layers previously dried at 70 ºC.

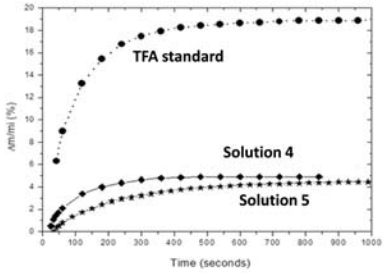

Figure 3. Water absorption in dried films versus time for TFA and 4 and 5 solutions

Our results demonstrate that low fluorine solutions produce less hygroscopic layers than TFA solutions. The absorption of water is reduced from 18% for the TFA solution to 4% for the low fluorine solutions 4 and 5. These results can be explained by the presence of coordination compounds (TEA or Propionic acid) of the metal salts, which therefore prevents their coordination with water molecules (Scheme 3). The presence of dimeric systems in solution for Copper and Yttrium [30] favours free coordination positions to be occupied by water molecules.

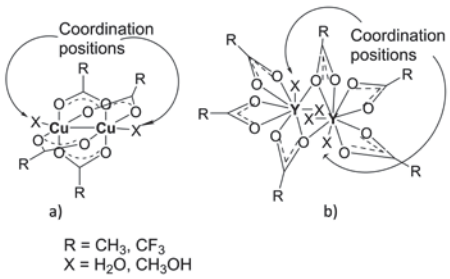

Scheme 3. Representation of the coordination positions for (a) Copper and (b) Yttrium compounds in solution.

309
310 *3.4. Thermogravimetric and evolved gas analysis.*
311
312 Customarily, TG analysis is done using powders. However, in a recent work, relevant
313 differences were observed when the analysis was performed in films [31]. Films are
314 expected to decompose differently than powders when the decomposition is controlled
315 by: a) transport of reactive gas, b) evolution of gaseous species or c) heat transport out
316 of the sample. All these aspects are not exclusive of decomposition processes but are
317 intrinsic to most solid-gas reactions[32].. In previous papers it has been shown that, for
318 several precursors, significant differences between powders and films arise [33–35]. So,
319 it is clear that optimization of the pyrolysis step cannot be achieved with thermal
320 analyses of powders.

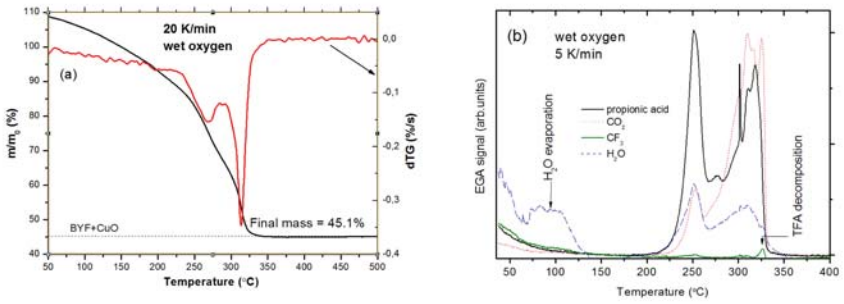

Figure 4. a) TGA and b) EGA analysis of the solution 5 in the form of thin film after spin coating deposition and drying. Both experiments were carried out under a dynamic wet oxygen atmosphere.

321
322 The evolution of the sample mass and of the evolved volatiles during pyrolysis
323 of the dried solution 5 is shown in Figure 4. In particular we observe the formation of
324 H_2O (m/z=18), propionic acid (m/z=29), CO_2 and CF_3CFO (m/z=69). In Figure 4 only

the evolution of the main fragments is shown but volatile identification is based on the complete analysis of the defragmentation pattern. TG curves are normalized to the mass of the sample once dehydrated, m_0. Since EGA analysis shows that dehydration is completed at 150ºC, the value of m_0 corresponds to that of the sample mass at 150ºC. The decomposition takes place in two consecutive stages that exhibit a maximum transformation rate at 265 and 310ºC respectively (see the time derivative of the TG curve). These two stages entail the decomposition of the propionate salts and the formation of propionic acid. At low temperature, the main volatile is propionic acid while at higher temperature CO_2 is the main volatile, mostly related to propionic acid decomposition in the gas phase. In addition, only traces of fragments related to acetic acid were observed, therefore EGA analysis confirms the scrambling between propionate and acetate radicals in the solution.

Assuming that the deposited solution contains YTFA, Barium and Copper propionates, the mass of the dehydrated solution should be m_0 = 406 mg per 1 mL of solution. According to Figure 1, after pyrolysis the solid residue is mainly BYF and CuO, therefore the mass of the solid residue at 500ºC is 184 mg per 1 mL of solution, i.e., 45.3% after normalization to m_0. From Fig. 4, one can verify a nice agreement between the predicted final mass (dashed line at 45.3%) and the measured final mass 45.1%. Notice that, in the case of a dried solution of YTFA, Barium and Copper acetates, the mass of the dehydrated solution would be m_0 = 371 mg per 1 mL and the mass after pyrolysis would be 41.0%, clearly in disagreement with the measured final mass.

To check the influence of the water on the reaction we have compared the TG curves obtained under wet and dry oxygen atmospheres (Figure 5.a). Apart from the fact that the initial water uptake is slightly smaller in dry conditions, the evolution of the reaction is very similar under both conditions, i.e., water does not affect the reaction behavior. Conversely, apart from CO_2, the main volatile detected under dry conditions by EGA is 3-pentanone. The main fragment of the fragmentation pattern of 3-pentanone is m/z=57, while in the case of propionic acid the intensity of the fragment m/z=57 is about half the intensity of fragment m/z=29 [36]. In wet conditions, we observe that fragment m/z=29 is about two times more intense than fragment m/z=57, but in dry conditions the more abundant fragment is m/z=57 (Figure 5.b). Actually, it is well known that propionate salts decomposition entails the release 3-pentanone [37,38]. Therefore, the formation of propionic acid observed under wet conditions may result from the reaction in the gas phase between the released 3-pentanone and the water present in the atmosphere.

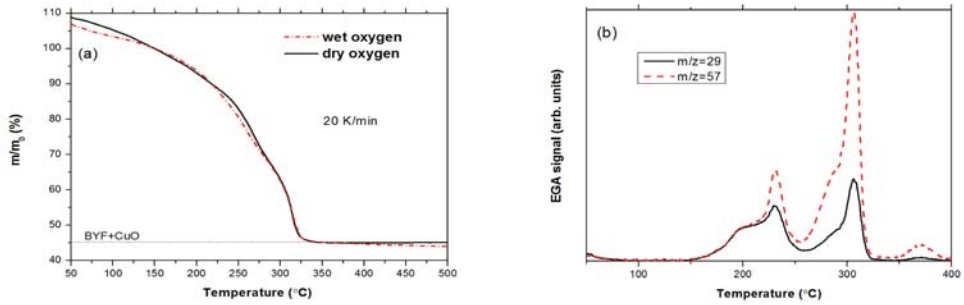

Figure 5 a) TGA analysis of the solution 5 under dry (dotted) and wet (solid) oxygen atmosphere and b) EGA analysis of fragments m/z=29 (solid) and 57 (dashed) of the solution 5 under wet oxygen atmosphere.

361
362 The DSC signal (Figure 6) shows two exothermic peaks nicely correlated to the
363 mass loss rate at the two decomposition stages. This result rules out the formation of
364 propionic acid being related to an evaporation reaction of propionic acid and clearly
365 indicates that precursor pyrolysis is an exothermic process.

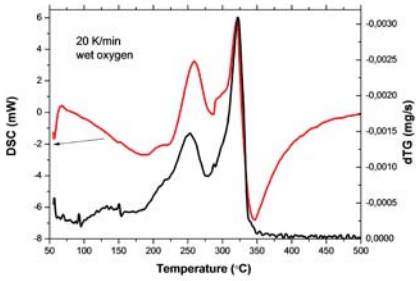

Figure 6. Simultaneous DSC and TGA analysis of the solution 5 in the form of thin film after spin coating deposition and drying. The dTG signals corresponds to the time derivative of the mass with respect time.

366
367 As for the TFA groups, the EGA curve in Fig 4.b shows a tiny signal around
368 320ºC that would correspond to the decomposition of YTFA. Note that the formation of
369 BYF involves that 72% of the fluorine atoms initially present on the solution should
370 remain in the film after pyrolysis; therefore, a weak signal related to fluorinated species
371 is in agreement with the formation of BYF.
372 The previous characterization is consistent with the FTIR *ex-situ* analysis of the solid
373 residue at different temperatures (Figure 7). The FTIR spectrum accounts for the

presence of TFA ligands in different bonding modes, most notably a strong broad absorption in the 1732–1622 cm^{-1} region centered at 1685 cm^{-1} and strong absorptions centered at 1208 cm^{-1} and 1150 cm^{-1} [39,40]. Propionate ligands exhibit absorption peaks at 2978 cm^{-1}, 2944 cm^{-1} and 2876 cm^{-1}, a strong broad band centered at 1568 and absorption peaks at 1466 cm^{-1}, 1431 cm^{-1}, 1371 cm^{-1} and 1299 cm^{-1} [36]. In addition, a broad band in the 3050–3700 cm^{-1} region centered at 3433 cm^{-1} is related to water[39,41]. FTIR spectra show a progressive diminution of the absorption peaks related to propionate groups from 200ºC up to 300ºC while TFA absorption peaks remain unaffected up to 300ºC, and at 320ºC there is a significant diminution of the amplitude of TFA absorption peaks. Note also that the amplitude of the broad band centered at 3433 cm^{-1} and related to H_2O remains roughly constant up to 300ºC. Since FTIR analysis is performed *ex-situ* this indicates that up to 300ºC films are very hygroscopic i.e., after a short exposure to ambient, films take up water. Since the presence of propionic groups clearly diminishes from 200 to 300ºC while TFA group remain roughly constant, this would indicate that these solutions are highly hygroscopic mainly due to the presence of YTFA. Indeed, TFA salts and in particular YTFA is very hygroscopic due to its high Lewis acidity [39,42]. This fact would also account for the lower water uptake of these low fluorine solutions when compared to standard TFA solutions (Figure 2).

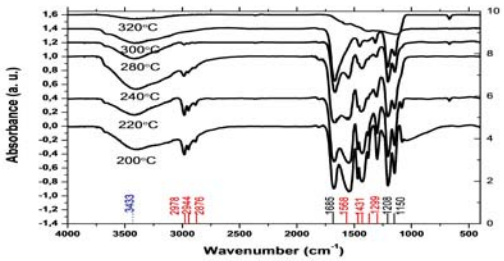

Figure 7. FTIR spectra of the film from solution 5 after heating it to a given temperature in humid oxygen. Bottom x axis: in black, red and blue (dotted) the absorption peak positions related to TFA ligands, propionate ligands and water, respectively.

It is worth noting that despite the fact that TFA salts decompose at the very end of the precursor pyrolysis, no barium carbonate is formed. Indeed, EGA analysis shows that most fluorine remains after precursor pyrolysis and XRD exhibits the formation of BYF and no traces of $BaCO_3$ are detected (Fig. 8). Moreover EGA analysis performed up to 830ºC shows no traces of CO_2, that would result from the decomposition of $BaCO_3$. Instead, at 550ºC we observe the formation of fluorine volatiles related to BYF decomposition to form Y_2O_3 and BaF_2. Therefore, the use of BaTFA is not compulsory to prevent $BaCO_3$ formation, adding the fluorine amount necessary to form BYF may

suffice.

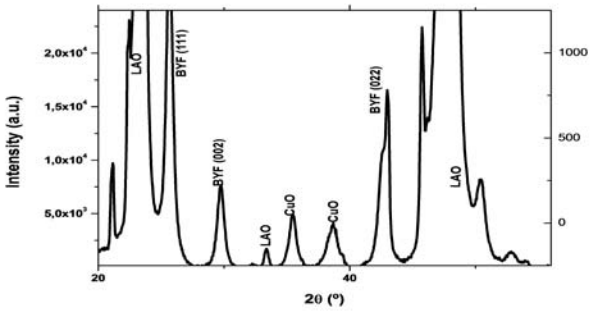

Figure 8. Solution 4. XRD after pyrolisis showing similar pattern than standard TFA solution

3.5. Thermal treatment.

Upon all the analysis performed and reasons exposed up to now for the different solutions investigated, we decide to use mainly solution 4 for the growth of YBCO layers. The solution was deposited by spin coating on LAO single crystal and the decomposition of the metallorganics was achieved at rather low temperature, and then a high temperature treatment until the maximum growth temperature (800-820ºC) was pursued.

The pyrolysis for the solution **4 and 5**was done between 100 and 500ºC using humid oxygen atmosphere.

X-Ray diffraction analysis of solution 4 pyrolyzed sample showed crystalline phases corresponding to Copper Oxide and (Barium,Yttrium) fluorides (see figure 8). The reduction of fluorine content in the precursor solution does not seem to affect the final aspect and composition of the pyrolized layer. Neither barium carbonate nor other

phases were detected. ISCD file numbers for XRD analysis are in the reference [43]

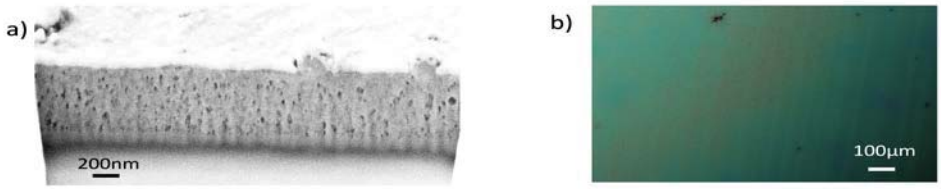

Figure 9. (a) FIB cross section image and (b) Optical Microscopy image of a YBCO film prepared from solution 4 after pyrolisis at 500ºC

Smooth pyrolyzed layers are achieved after the thermal treatment at 500ºC using humid O_2 (but also with air atmosphere). Formation of vertical open porosity is observed (Fig. 9) by FIB analysis. Due to the films morphology and taking into account their poor mechanical properties at this stage [14], this vertical open porosity is attributed to gas escape towards the film surface.

3.6. Characterization of epitaxially grown films

Considering the growth mechanism of YBCO films in the TFA approach which essentially proceeds through the reaction of $Ba(O_xF_y)_2$, CuO and Y_2O_3, we should not expect major modifications of the optimal processing conditions [44] using the low fluorine solutions. Therefore, the pyrolyzed films were grown at 820ºC, in a humid N_2 atmosphere with 200 ppm O_2 [18, 19]. After growth, the thickness ranged from 250 to 350 nm depending on the concentration and viscosity of the solution. The films were systematically analyzed by XRD and SEM (Figure 10) for solution **4**, to respectively check the epitaxial quality and the morphology at the nanometric scale. The θ–2θ XRD pattern showed that YBCO films only have (00l) reflections and that no secondary phases are present. The films display a sharp texture, as identified by narrow in-plane ϕ-scan values, $\Delta\phi$=0.5º and rocking curves $\Delta\omega$ = 0.2º. A typical case for solution **4** is presented in Figure 10. All these structural analysis results are comparable to those from the standard TFA solution and SEM images showed also homogeneous and rather compact layers (Figure 10b), however a detailed intermediate phase evolution analysis [45] together with a TEM study of the microstructure should be carried out to ascertain if the defect structure is modified [46].

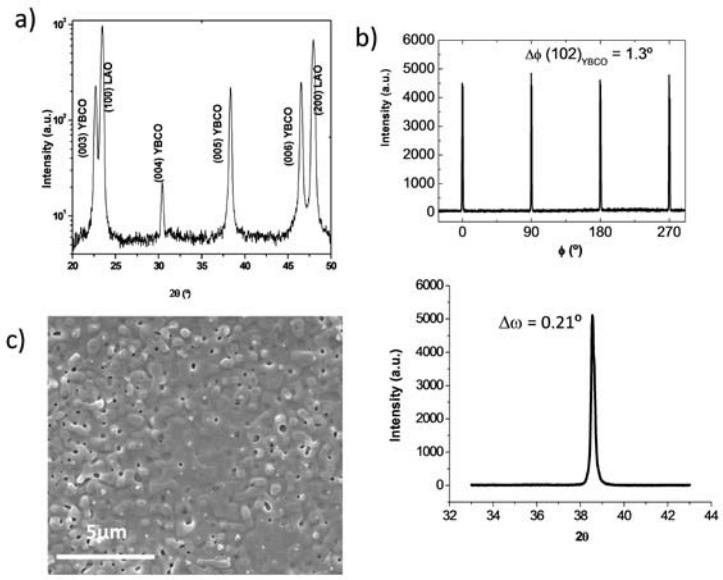

Figure 10. (a) XRD q-2q analysis (b) phi-scan and rocking curve (c) SEM image of the YBCO layer formed from solution 4 after growth on LAO.

The superconducting properties seem to be more sensitive to the particular solution. In general, J_c(77K)= 3-4 MA/cm^2 at self-field and T_c = 92 K, were measured by SQUID magnetometer which are in the same range of values than those obtained using our standard TFA process[6] . In Figure 11, a plot of the critical current density, J_c(self-field, 77 K) versus different solutions for layers with similar thickness (~300 nm) is shown. The best results, comparable with standard TFA solution (0 in the graph) are obtained using solutions 3, 4 and 5. However, we must remind that the reproducibility of solution 3 was rather poor due to the deposition difficulties explained before.

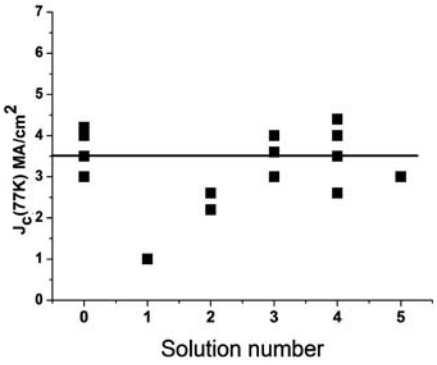

Figure 11. J_c(77K) of the YBCO films grown via low-fluorine solutions 1 to 5 for different samples. Solution zero corresponds to TFA standard solution and solutions 1 to 5 are those indicated in Table 2

We have completed the analysis of the superconducting properties of a YBCO film at 77 K grown with solution 4 by means of in-field angular transport measurements. Figure 12 shows the comparison between a sample J_c^{sf}(77 K) = 4.3 MA/cm^2 grown with standard TFA solution and a sample with J_c^{sf}(77 K) = 4.4 MA/cm^2 grown with solution 4. Very similar results are obtained for both J_c(H) and J_c(θ) dependencies indicating that they present comparable vortex pinning properties and thus similar microstructural defects. The two anisotropic peaks J_c(θ) associated to twin boundaries (at θ=180º for H//c) and mainly stacking faults (at θ=90º for H//ab) are also very similar. We therefore conclude that the low fluorine solutions, and solution 4 in particular, is able to obtain high performance YBCO films following a fluorine-based CSD growth.

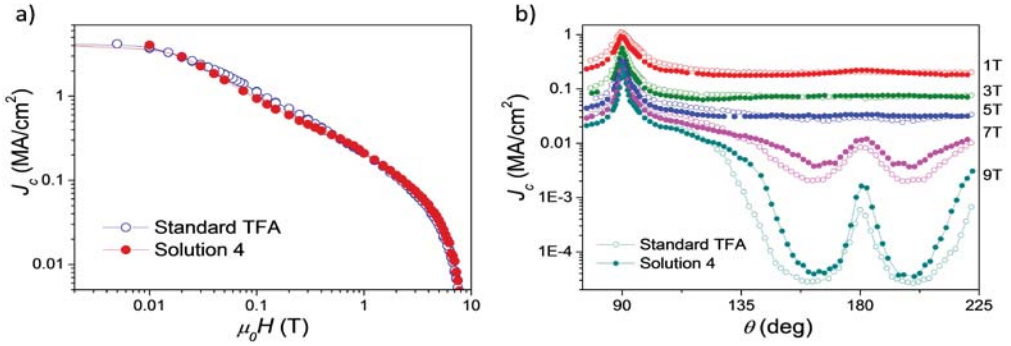

Figure 12. (a) Magnetic field dependence at H//c and (b) angular dependence at several fields of the critical current density at 77K for a YBCO sample grown with a TFA solution and a sample grown with solution 4.

From all the results presented in this paper, we can suggest that solutions 4 is the most suitable one to fulfill all the requirements of environmental safety and robustness, and reaching good structural and superconducting properties.

4. Summary

The chemistry involved in the preparation of YBCO solutions with reduction of fluorine content has been studied and a set of different stable low fluorine solutions has been proposed (decreasing the fluorine content even down to 10%). These solutions produced layers that after deposition and drying are less hygroscopic and more robust towards environmental conditions. This fact can be related to the presence of coordinating ligands (carboxylic and aminoalcohols) that hampers the absorption of water due to the reduced amount of TFA ligands. Among the solutions analyzed, the ones with 20% of fluorine have been more deeply studied. It has been observed that decomposition is an exothermic process and proceeds through two stages that involve the decomposition of propionic salts and the release of 3-pentanone. No volatiles related to acetates have been detected by EGA, i.e., during solution in propionic acid, Ba and Cu acetate transform into Ba and Cu propionates, as also confirmed by NMR analysis. At the end of the last stage, around 320ºC YTFA decomposes, being the final solid residue after pyrolysis mainly BYF and CuO. During pyrolysis only small amounts of volatiles containing fluorine have been observed, i.e., after pyrolysis most fluorine remains in the solid residue to form BYF. Pyrolysis is completed at 350ºC for all low fluorine solutions. After deposition on LAO and the growth process, YBCO epitaxial layers layers of around 300 nm were obtained presenting high structural and superconducting properties, similar to those obtained for standard TFA solution**.**

Acknowledgements

The authors acknowledge the financial support from MICINN (Consolider NANOSELECT, CSD2007-00041, MAT 2011-28874-C02, MAT2014-51778-C2-2-R); Generalitat de Catalunya (Pla de Recerca 2014-SGR-753 and XaRMAE), and EU (FP7 NMP-LA-2012-280432 EUROTAPES project and MP1201 Cost action).

References

[1] Foltyn S R, Civale L, Macmanus-Driscoll J L, Jia Q X, Maiorov B, Wang H and Maley M 2007 *Nat. Mater.* **6** 631–42

[2] Obradors X and Puig T 2014 *Supercond. Sci. Technol.* **27** 044003

[3] Chen D-X, Pardo E, Sanchez A, Bartolomé E, Puig T and Obradors X 2007 *Appl. Phys. Lett.* **90** 072501

[4] Shiohara Y, Taneda T and Yoshizumi M 2012 *Jpn. J. Appl. Phys.* **51** 010007-16

[5] Rupich M W, Li X, Thieme C, Sathyamurthy S, Fleshler S, Tucker D, Thompson E, Schreiber J, Lynch J, Buczek D, DeMoranville K, Inch J, Cedrone P and Slack J 2009 *Supercond. Sci. Technol.* **23** 014015

[6] Obradors X, Puig T, Ricart S, Coll M, Gazquez J, Palau A and Granados X 2012 *Supercond. Sci. Technol.* **25** 123001

[7] Llordés A, Zalamova K, Ricart S, Palau A, Pomar A, Puig T, Hardy A, Van Bael M K and Obradors X 2010 *Chem. Mater.* **22** 1686–94

[8] Erbe M, Hänisch J, Freudenberg T, Kirchner A, Mönch I, Kaskel S, Schultz L and Holzapfel B 2014 *J. Mater. Chem. A* **2** 4932

[9] Zalamova K, Pomar A Palau A, Puig T and Obradors X 2009 I *Supercond. Sci. Technol.* **23** 014012

[10] Coll M, Guzman R, Garcés P, Gazquez J, Rouco V, Palau A, Ye S, Magen C, Suo H, Castro H, Puig T and Obradors X 2014 S *Supercond. Sci. Technol.* **27** 044008

[11] Horide T, Kawamura T, Matsumoto K, Ichinose A, Yoshizumi M, Izumi T and Shiohara Y 2013 J *Supercond. Sci. Technol.* **26** 075019

[12] Morlens S, Romà N, Ricart S, Pomar A, Puig T and Obradors X 2007 *J.Mat. Res.* **22** 2330-38

[13] Wu W, Feng F, Shi K, Zhai W, Qu T, Huang R, Tang X, Wang X, Hu Q, Grivel J-C and Han Z 2013 *Supercond. Sci. Technol.* **26** 055013

[14] Zalamova K, Roma N, Pomar A, Morlens S, Puig T, Carrillo A E, Sandiumenge F, Ricart S, Obradors X and Uab C De 2006 *Chem. Mat.***18** 5897-5906.

[15] Chen Y, Wu C, Zhao G and You C 2012 *Supercond. Sci. Technol.* **25** 069501

[16] Armenio a A, Augieri A, Ciontea L, Contini G, Davoli I, Giovannantonio M Di, Galluzzi V, Mancini a, Rufoloni a, Petrisor T, Vannozzi A and Celentano G 2011 *Supercond. Sci. Technol.* **24** 115008

[17] Romà N, Ricart S, Moretó J M, Morlens S, Castaño O, Pomar a, Puig T and Obradors X 2006 *J. Phys. Conf. Ser.* **43** 178–81

[18] Calleja a., Ricart S, Palmer X, Luccas R F, Puig T and Obradors X 2009 *J. Sol-Gel Sci. Technol.* **53** 347–52

[19] Bean C P 1962 *Phys.Rev.Lett.* **8** 250–3

[20] Sanchez A and Navau C 2001 *Phys. Rev. B* **64** 214506

[21] Sathyamurthy S, Tuncer E, More K L, Gu B, Sauers I and Paranthaman M P 2012 *Appl. Phys. A* **106** 661–7

[22] Hansen C M 2004 50 *Prog. Org. Coatings* **51** 77–84

[23] Hubert-Pfalzgraf L G 2003 *Inorg. Chem. Commun.* **6** 102–20

[24] Van Driessche I, Feys J, Hopkins S C, Lommens P, Granados X, Glowacki B a, Ricart S, Holzapfel B, Vilardell M, Kirchner a and Bäcker M 2012 *Supercond. Sci. Technol.* **25** 065017

[25] Vilardell M, Granados X, Ricart S, Van Driessche I, Palau A, Puig T and Obradors X 2013 *Thin Solid Films* **548** 489–97

[26] Cheng A T and Howald R 1968 *Inorg. Chem.* **7** 2100–5

[27] Whitmire K H, Hutchison J C, Gardberg A and Edwards C 1999 *Inorganica Chim. Acta* **294** 153–62

[28] Xu G, He X, Lv J, Zhou Z, Du Z and Xie Y 2012 *Cryst. Growth Des.* **12** 3619–30

[29] Mishra S, Zhang J, Hubert-Pfalzgraf L G, Luneau D and Jeanneau E 2007 *Eur. J. Inorg. Chem.* **2007** 602–8

[30] Schubert U 2005 *J. Mater. Chem.* **15** 3701

[31] Roura P, Farjas J, Eloussi H, Carreras L, Ricart S, Puig T and Obradors X 2015 *Thermochimica Acta* **601** 1–8

[32] Farjas J, Pinyol a., Rath C, Roura P and Bertran E 2006 *Phys. Status Solidi* **203** 1307–12

[33] Sanchez-Rodriguez D, Farjas J, Roura P, Ricart S, Mestres N, Obradors X and Puig T 2013 T *J. Phys. Chem. C* **117** 20133–8

[34] Roura P, Farjas J, Ricart S, Aklalouch M, Guzman R, Arbiol J, Puig T, Calleja a., Peña-Rodríguez O, Garriga M and Obradors X 2012 *Thin Solid Films* **520** 1949–53

[35] Eloussifi H, Farjas J, Roura P, Ricart S, Puig T, Obradors X and Dammak M 2013 T *Thin Solid Films* **545** 200–4

[36] *NIST Chem. Webbook, http//webbook.nist.gov/cgi/cbook.cgi?ID=C79094&Units=SI&Mask=200#Mass-Spec, http//webbook.nist.gov/cgi/cbook.cgi?ID=C96220&Units=SI&Mask=200#Mass-Spec (accessed June 2015).*

[37] Barnes P A, Stephenson G and Warrington S B 1982 *J. Thermal Anal.* **25** 299–311

[38] Grivel J C 2013 *J. Anal. Appl. Pyrolysis* **101** 185–92

[39] Mishra S, Hubert-Pfalzgraf LG, Daniele S, Rolland M, Jeanneau E J B 2009 *Inorg. Chem. Commun.* **12** 97-100

[40] Gibson DH, Ding Y, Miller RL, Sleadd BA, Mashuta MS R J 1999 *Polyhedron.* **18** 1189–200

[41] H. Eloussifi, J. Farjas, P. Roura, J. Camps, M. Dammak, S. Ricart et al. 2012 *J. Therm. Anal. Calorim.* **108** 589–96.

[42] Zhang J, Morlens S, Hubert-Pfalzgraf LG L D 2005 Eur. J. *Inorg Chem* 3928–35

[43] ISCD files [00-048-1548] for CuO, [00-004-0452] for BF, [00-046-0039] for BYF, [00-011-0697] for $BaCO_3$ and [00-041-1105] for Y_2O_3.

[44] Gazquez J., Sandiumenge F., Coll M., Pomar A., Mestres N., Puig T., Obradors X., Kihn Y., Casanove M. J., 2006 *Chem. Mater.* **18** 6211–9

[45] Chen H, Zalamova K, Pomar a, Granados X, Puig T and Obradors X 2010 *Supercond. Sci. Technol.* **23** 034005

[46] Pomar A, Llordés A, Gibert M, Ricart S, Puig T and Obradors X 2007 *Phys. C Supercond.* **460-462** 1401–4